ANALYTICAL STUDY OF THE EXCESS ENTHALPY IN THE COMBUSTION WITHIN POROUS MEDIA

Fernando Marcelo Pereira
Department of Mechanical Engineering
Federal University of Santa Catarina
Florianópolis - SC
fernando@cet.ufsc.br

Amir Antonio Martins Oliveira
Department of Mechanical Engineering
Federal University of Santa Catarina
Florianópolis - SC
amirol@emc.ufsc.br

Abstract. This work analyses theoretically the excess enthalpy for laminar free flames and for flames within porous media in order to estimate the amount of excess temperature originated by the presence of the porous matrix and the factors that affect it. The analysis is based on the excess enthalpy function previously defined in the literature applied to the non-dimensional volume-averaged equations for the combustion within an inert porous medium. Approximations for the reactants and the solid temperature profiles are assumed and the dependence of the excess enthalpy function on the problem parameters is accessed. The results obtained are in good qualitative agreement with numerical results. The excess enthalpy is shown to be a function of the gas Lewis number, the ratio of the solid- and the gas-phasic effective thermal conductivities and the porosity of the medium.

Keywords. *superadiabatic combustion, porous media, excess enthalpy, thermal and chemical non-equilibrium.*

1. Introduction

The combustion in porous media has received much attention in the last decades as a way of extending flame stability, burning fuel lean mixtures and providing radiant heating. The heat recirculation induced by the porous media adds to the energy released by combustion resulting in local temperatures in excess of the adiabatic flame temperature for the gas phase, a phenomenon that has been called superadiabatic combustion (Echigo et al., 1991). This high temperature in the reaction region increases the reaction rate and allows for combustion of low heat content gas mixtures whose stoichiometric ratio lies under the flammability limit in laminar free flames. The amount of excess temperature within the porous medium depends on the thermal properties of the gas and solid phases and has not been yet shoed explicitly as a function of thermal properties.

The increased thermal radiation emission from the flame within the porous medium led to the development of efficient radiant burners. These equipments have been used in industrial applications that need controlled and sometimes staged superficial heating. Each application requires different solutions in terms of power, operational temperature and burner shape. The burner temperature must also remain under the matrix maximum operational temperature to prevent matrix degradation. Since the stability range and radiant efficiency of these burners are functions of the burner configuration and the heat loss, the flame behavior under each condition changes. Then it is necessary to introduce new burner designs to face different applications.

Most numerical models for the simulation of this problem requires the simultaneous solutions of chemical kinetics, thermal energy and hydrodynamic equations. The stiffness and nonlinearity of the chemical reaction terms combined with the nonlinearity of the flow in porous media brings difficulties in building useful design tools to the development of new burners because of the large computational effort involved. Simplified models that could quickly predict just the most important aspects of the combustion within a porous media would be of great interest.

Some researchers have focused their attention on developing new schemes to solve the reacting flows in a less expensive manner. Goey and Boonkkamp (1999) developed a flamelet-generated-manyfold (FGM) method where a higher dimensional flame is considered as an ensemble of one-dimensional flames. In this model, the flame is divided in three parts: one part describes the fluid motion and mixing process, a second part describes the front motion through a kinematic G-equation and a third part consists of a set of 1D flamelet equations, using a local coordinate adapted to the flame sheet, governing the inner flame structure and local mass burning rate. The flamelet equations are solved treating the system as a 1D adiabatic premixed flame. These solutions form a manifold that can be used in subsequent simulations. To test this method they simulated a ceramic-foam surface burner in a radiating furnace and compared the results with experiments. The small differences between computed and measured temperatures were within the experimental error.

Bielert and Sichel (1998) developed a volume fraction based front tracking method and solved an unsteady one-dimensional turbulent flame. Their model does not compute the details of chemical kinetics, turbulence generation and dissipation and turbulent flame interactions. They assumed that the reaction occurs within a thin combustion front propagating into the unreacted fuel/oxidizer mixture. The flame front velocity, which does depend on flame kinetic and

turbulence interaction, is calculated with an algebraic model based on the laminar flame velocity with an empirical extension for the influence of turbulence fluctuations. They showed that this method can reproduce experimental results over a wide range of combustion conditions in a closed tube, such as fast acceleration of flames followed by transition to detonation (ethylene/oxygen mixtures) or slow combustion (methane/air flames).

Following the same idea, the use of a flame tracking method in combination with analytical expressions that describe the temperature gradients at the reaction zone and the flame velocity, without the need for solving the complex reaction rates, can be an interesting way of accessing the main aspects of the combustion in porous media and of building a useful design tool for burners with complex three-dimensional shapes.

In this work we propose an analytical solution for the one-dimensional conservation equations for energy and chemical species using a two-medium model based on Sahraoui and Kaviany (1994) and the excess enthalpy function previously defined in the literature. Approximations for the reactants and the solid temperature profiles are assumed and the dependence of the excess enthalpy function and excess temperature on the problem parameters is accessed.

This analysis is the first step in the construction of a sub-grid model to be coupled with a front tracking method. The aim of this sub-grid model is to reproduce the most important aspects of the flame front within a porous medium as the front velocity, the gas and the solid temperature profiles and the superadiabatic temperature.

2. Model Formulation

A one-dimensional, two-medium model for the conservation of mass, gas phase energy, solid phase energy and species is written following Sahraoui and Kaviany (1994). The mass conservation implies that $\rho_n u_n$ is constant for the one-dimensional flow with ρ_n and u_n being respectively the gas density and the gas velocity far upstream from the flame. For a steady state, stationary flame, the laminar flame speed S_L is equal to u_n. The specific heat capacity c_p, the thermal conductivities (λ_g for the gas and λ_s for the solid) and the product ρD (density times mass diffusivity) are assumed uniform along the flame. The gas and solid radiation and the dispersion effects are neglected. For highly porous ($\varepsilon > 0.75$), large pores ($Dp > 0.1$ mm) porous media, the pressure along the porous medium is approximately uniform, and the momentum equation becomes trivial. The thermal conductivities and the mass diffusivity are effective properties in the respective phase (i.e., include the pore channel variable area and tortuosity effects; Kaviany, 1995). A single-step, first-order in the fuel concentration and zeroth-order in the oxidant concentration, Arrhenius reaction rate is adopted (although not accurate, allows for a simple analysis). The steady state, volume-averaged energy and species conservation equations (omitting for simplicity the volume-averaging notation) then become:

$$\varepsilon\rho_n u_n \frac{dY_F}{dx} = \varepsilon\rho D \frac{d^2Y_F}{dx^2} - \varepsilon w \qquad (1)$$

$$\varepsilon\rho_n u_n c_p \frac{dT_g}{dx} = \varepsilon\lambda_g \frac{d^2T_g}{dx^2} + \varepsilon wQ + h_v\left(T_s - T_g\right) \qquad (2)$$

$$0 = (1-\varepsilon)\lambda_s \frac{d^2T_s}{dx^2} - h_v\left(T_s - T_g\right) \qquad (3)$$

$$w = AT_g^a \nu_F \rho Y_F \exp\left(\frac{-\Delta E_a}{R_g T_g}\right) \qquad (4)$$

where ε is the porosity of the solid matrix, Q is the fuel mass based heat of reaction, $h_v = S_{gs}h$, is the volumetric convection coefficient, S_{gs} is the interfacial specific area between the solid and the gas phases (m^2/m^3), $h = Nu\lambda_{s,m}/D_p$ is the local convection coefficient with, Nu, D_p and $\lambda_{s,m}$ being respectively the averaged Nusselt number for a fully developed flow through a porous medium, the mean pore diameter of the solid matrix and the molecular thermal conductivity of the gas phase, ΔE_a is the activation energy and R_g is the universal gas constant.

Defining the following non-dimensional fuel mass fraction, temperature and spatial coordinate (Williams, 1985),

$$y = \frac{Y_F}{Y_{F,n}}, \quad \theta = \frac{c_p\left(T - Tn\right)}{Y_{F,n}Q} = \frac{T - T_n}{T_r - T_n}, \quad \zeta = \int_0^x \frac{\rho_n u_n c_p}{\lambda_g} dx \qquad (5)$$

the non-dimensional equations become:

$$\varepsilon\frac{dy}{d\zeta}=\varepsilon\left(\frac{1}{Le}\right)\frac{d^2y}{d\zeta^2}-\varepsilon DaW \qquad (6)$$

$$\varepsilon\frac{d\theta_g}{d\zeta}=\varepsilon\frac{d^2\theta_g}{d\zeta^2}+\varepsilon DaW+N\left(\theta_s-\theta_g\right) \qquad (7)$$

$$0=\Gamma_s\left(1-\varepsilon\right)\frac{d^2\theta_s}{d\zeta^2}-N\left(\theta_s-\theta_g\right) \qquad (8)$$

The non-dimensional parameters appearing in the volume-averaged conservation equations are:

$$Le=\frac{\lambda_g}{\rho c_p D} \qquad Da=\frac{A_0\nu_F T_g^a \rho e^{\frac{-\beta}{\alpha}}\lambda_g}{\rho_n^2 u_n^2 c_p} \qquad W=y\exp\left[\frac{-\beta\left(1-\theta_g\right)}{1-\alpha\left(1-\theta_g\right)}\right]$$

$$\beta=\alpha\frac{E_a}{R_g T_r}=\frac{E_a\left(T_r-T_n\right)}{R_g T_r^2} \qquad \alpha=\frac{QY_{F,n}}{c_p T_r}=\frac{T_r-T_n}{T_r} \qquad \Gamma_s=\frac{\lambda_s}{\lambda_g}$$

$$N=\frac{\lambda_g h_v}{\left(\rho_n u_n c_p\right)^2} \qquad (9)$$

In these equations Le is the Lewis number, Da is the Damköhler number, W is the non-dimensional reaction rate, β is the Zel'dovich number, α is the enthalpy ratio, Γ_s is the ratio between the solid and gas thermal conductivities and N is the interfacial heat transfer parameter. The parameters Le, β and α are constants that depend upon the initial conditions and the constant properties assumed in the model. The parameter N is assumed to be independent of θ_g.

Summing Eqs. (6), (7) and (8) up, we find:

$$\frac{d\left(y+\theta_g\right)}{d\zeta}=\frac{d^2}{d\zeta^2}\left[\frac{y}{Le}+\theta_g+\Gamma_s\left(\frac{1}{\varepsilon}-1\right)\theta_s\right] \qquad (10)$$

The overall energy balance $c_p(T-T_n) = Q(Y_{F,n}-Y_F)$ is non-dimensionalized to give $y + \theta_g = 1$. Then, one can define a new variable $H = y + \theta_g - 1$, called excess enthalpy function. This function accounts for the total enthalpy of the gas, including the thermal and chemical enthalpies. From the definition of H, Eq. (10) is rewritten as:

$$\frac{dH}{d\zeta}=\frac{d^2H}{d\zeta^2}+\underbrace{\left(\frac{1}{Le}-1\right)\frac{d^2y}{d\zeta^2}}_{S_{ff}}+\underbrace{\Gamma_s\left(\frac{1}{\varepsilon}-1\right)\frac{d^2\theta_s}{d\zeta^2}}_{S_{pm}} \qquad (11)$$

When ε = 1 we recover a laminar free flame and when Le = 1 the enthalpy function is conserved. Otherwise, the H equation will have a positive or negative source term depending on the signs for the diffusion-like terms involving the non-dimensional fuel fraction and solid temperature distributions. The second term in the right hand side of the Eq. (11) - called free flame source term S_{ff} - accounts for the ratio between the mass and thermal diffusion thicknesses. The third term - called porous media source term S_{mp} - accounts for the effect of the solid matrix. The overall result in the H distribution in the flame zone will depend on the relative magnitudes of these terms.

3. Approximated Closed Form Solution for the Excess Enthalpy Function

The origin of the coordinate axis is set to coincide with the flame front, i.e., the point where the fuel concentration reaches zero. Equation (11) is subjected to the following upstream and downstream boundary conditions:

$$\zeta \to -\infty ; \begin{bmatrix} y = 1 \\ \theta_g = \theta_s = 0 \\ H = 0 \\ d/d\zeta = 0 \end{bmatrix} \quad , \ \zeta = 0 ; \begin{bmatrix} y = 0 \\ \theta_s = \theta_0 \\ H = H_0 \end{bmatrix} \quad \zeta \to +\infty ; \begin{bmatrix} y = 0 \\ \theta_g = \theta_s = 1 \\ H = 0 \\ d/d\zeta = 0 \end{bmatrix} \qquad (12)$$

where θ_0 and H_0 are the values of the solid temperature and the excess enthalpy function at the origin.

Integrating Eq. (11) and applying the boundary conditions at $\zeta \to$ -∞, we obtain:

$$\frac{dH}{d\zeta} - H = \left(1 - \frac{1}{Le}\right)\frac{dy}{d\zeta} + \Gamma_s \left(1 - \frac{1}{\varepsilon}\right)\frac{d\theta_s}{d\zeta} \qquad (13)$$

Equation (13) is a linear non-homogeneous first order ordinary differential equation and is solved using an integration factor equal to $e^{-\zeta}$. To perform this integration, approximations for the fuel concentration and solid temperature are introduced – Eq.(14) and Eq.(15). These approximations are based on the solutions of equations (1) and (3) setting the reaction term to zero with the same boundary conditions of Eq.(12).

$$y = \begin{cases} 1 - e^{Le\zeta} ; \ at \ \zeta < 0 \\ 0 \quad\quad ; \ at \ \zeta > 0 \end{cases} \qquad (14)$$

$$\theta_s = \begin{cases} \theta_0 e^{m\zeta} \quad\quad\quad ; \ at \ \zeta < 0 \\ m\left(1 - \theta_0\right) e^{-m\zeta} \ ; \ at \ \zeta > 0 \end{cases} \qquad (15)$$

where m is a fin like parameter expressed as:

$$m = \left(\frac{N}{\Gamma_s \left(1 - \varepsilon\right)}\right)^{\frac{1}{2}} \qquad (16)$$

Figure (1) shows the profiles generated by these approximations. A limitation of Eqs.(14) and (15) is that for the θ_s profile the derivative will be continuous only when $\theta_0 = 0.5$ and for the y profile it will never be as y falls to zero at $\zeta = 0$. These simplifications will limit the accuracy of the analytical solution but will make it possible to obtain a simple closed form solution for the H equation. With the solid temperature and fuel concentration profiles approximation one can explicitly obtain the source terms of Eq.(11) as shown below.

$$S_{ff} = \begin{cases} Le\left(Le - 1\right) e^{Le\zeta} \quad ; to \ \zeta < 0 \\ 0 \quad\quad\quad\quad\quad\quad ; to \ \zeta > 0 \end{cases} \qquad (17)$$

$$S_{pm} = \begin{cases} \Gamma_s \left(\frac{1}{\varepsilon} - 1\right) m^2 \theta_0 e^{m\zeta} \quad\quad\quad ; to \ \zeta < 0 \\ \Gamma_s \left(\frac{1}{\varepsilon} - 1\right) m^2 \left(\theta_0 - 1\right) e^{-m\zeta} \quad ; to \ \zeta > 0 \end{cases} \qquad (18)$$

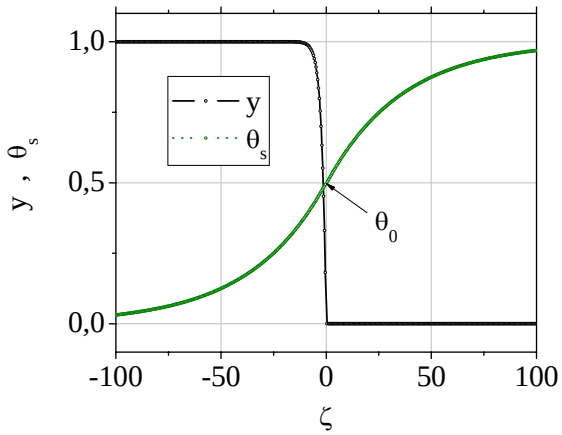

Figure 1. Non-dimensional fuel fraction and solid temperature approximations used in the solution of the H equation (here θ_0 = Le = 0.50). The other parameters are presented in Table 1.

Integrating Eq. (13) and applying the other boundary conditions, the solution for the excess enthalpy function is found as follows.

$$H = \begin{cases} \left(e^{\zeta} - e^{Le\zeta}\right) + \Gamma_s\left(\frac{1}{\varepsilon} - 1\right) m\left[\frac{\theta_0}{m-1}\left(e^{\zeta} - e^{m\zeta}\right) + \frac{1-\theta_0}{m+1}e^{\zeta}\right] & ;\ to\ \zeta < 0 \\ \Gamma_s\left(\frac{1}{\varepsilon} - 1\right)\left(1-\theta_0\right)\frac{m}{m+1}e^{-m\zeta} & ;\ to\ \zeta > 0 \end{cases} \qquad (19)$$

The first term of the right hand side of Eq(19) for $\zeta < 0$ accounts for the excess or defect of enthalpy generated by a Lewis number different from unity (free flame effect). The second term of the right hand side of Eq(19) for $\zeta < 0$ and the equation for $\zeta > 0$ account for the excess of enthalpy generated by the presence of the solid matrix in the reaction region.

The value of the H at $\zeta = 0$ (H_0) is easily calculated as shown in Eq.(20). This position corresponds to the maximum gas temperature because the fuel concentration reaches zero and liberates all its chemical energy. With Eq.(20) and the definition of H it is possible to find an explicit equation for the superadiabatic gas temperature T_{sup} as function of the solid temperature at the origin $T_{s,0}$ which is not known, and parameters of the problem. Equation (21) shows this expression in the form of a reduced temperature Θ. The superadiabatic temperature increases when the interfacial heat transfer parameter N or the thermal conductivity ratio Γ_s are increased but the analytical solution fails to converge when Γ_s tends to unity or when N or Γ_s tend to infinity. When the porosity is equal to unity (ε = 1), i.e., a gas phase free flame, or when there is no heat exchange between solid and gas (N = 0), T_{sup} equals the adiabatic flame temperature T_r.

$$H_0 = \Gamma_s\left(\frac{1}{\varepsilon} - 1\right)\left(1-\theta_0\right)\frac{m}{m+1} \qquad (20)$$

$$\Theta = \frac{T_{sup} - T_r}{T_r - T_{s,0}} = \Gamma_s \frac{\left(1-\varepsilon\right)}{\varepsilon}\sqrt{\frac{N}{N + \Gamma_s\left(1-\varepsilon\right)}} \qquad (21)$$

When the heat transfer between the gas and solid phases is set equal to zero (N = 0) or when the volumetric porosity is equal to unity, the excess enthalpy function reduces to the solution for a free flame as found in Vichman and Vance (1997), as shown in Eq.(22). When Le = 1 in Eq. (22), the excess enthalpy is conserved and H is equal to zero everywhere in the domain.

$$H = \begin{cases} e^{\zeta} - e^{Le\zeta} & ;\ to\ \zeta < 0 \\ 0 & ;\ to\ \zeta > 0 \end{cases} \qquad (22)$$

4. Results

In order to assess the accuracy of the approximate analytical solution obtained, equations (1), (2) and (3) were solved numerically for the methane-air system subjected to the boundary conditions of Eq. (12). The solution was obtained using a finite-volume method, with non-uniform, adapting grid and steps were taken to accelerate convergence to steady state. A total number of 301 grid points is used with a control volume thickness around 0,003 mm in the flame region. The flame speed (eigenvalue) was obtained from the overall mass balance. The algorithm was validated with the solution for a free flame with unity Lewis number and the experimental flame speeds for equivalence ratio of 1 and 0.5 for methane-air premixed combustion.

Table 1 shows the thermodynamic, transport and geometric properties of the solid and gas phases used and the corresponding non-dimensional parameters. The mean pore diameter is modeled as $D_p = (4\varepsilon/\pi)^{0.5}/(39.37\ PPI)$, which is a uniform pore distribution model, where PPI stands for pores per inch. Approximate values for the volumetric heat transfer coefficient h_v and the burner surface emissivity ε_b are used. The solid phase properties are taken from Möβauer et al. (1999).

Table 1. Thermodynamic, transport and geometric properties for the solid and gas (methane/air) phases and the corresponding non-dimensional parameters.

Gas Phase Properties		
Φ	1	-
T_n	298	K
T_r	2197	K
E_a	141E3	J/mol
A_0	2.2E8	1/s
R_g	8.314	J/mol-K
u_n	0.65	m/s
λ_g	0.082	W/m-K
ρ_n	1.2127	kg/m^3
c_p	1452	J/kg-K
Q	50144	kJ/kg $_{Fuel}$
ν_F	1	-
a	0	-

Solid Phase Properties		
λ_s	1 to 20	W/m-K
ε_b	0.8	-
PPI	10	ppi
L_q	0.10	m
D_p	2.56E-3	m
h_v	60E+3	W/m^{3}K

Non-dimensionals	
β	6.672
α	0.8644
Da	156.3
Γ_s	30.5 to 244
N	0.227
Re_D	9.884

The flame speed calculated by the analytical model depends strongly on the profiles assumed for the fuel mass fraction and solid temperature. The values obtained are usually 50% lower than the values obtained from the numerical calculations, making it difficult to correctly predict the inner structure of the flame. Therefore, in the analytical results shown below, the flame speed is considered known and the values calculated from the numerical solutions are used. This implies that the use of this model as a sub-grid model in future computations of complex flames will require an additional, perhaps, empirical adjustment for the local flame speed.

4.1. Flame Structure

Figure (2) shows numerical and analytical results for the non-dimensional gas and solid temperatures, fuel fraction and excess enthalpy distribution of a flame within a porous media with $\Phi = 1$, Le = 1, $\Gamma_s = 61$. In both solutions the non-dimensional gas temperature presents a peak that is more than 10% higher than the adiabatic flame temperature. The thermal flame thickness is wider than the fuel consumption thickness as a result of the large thermal conductivity of the solid phase. The enthalpy function presents an excess everywhere along the flame. The analytical solution reproduces qualitatively the same results of the numerical calculations. The major differences are found in the solid temperature profile as expected because of the imposed solid temperature at the origin ($\theta_0 = 0.5$).

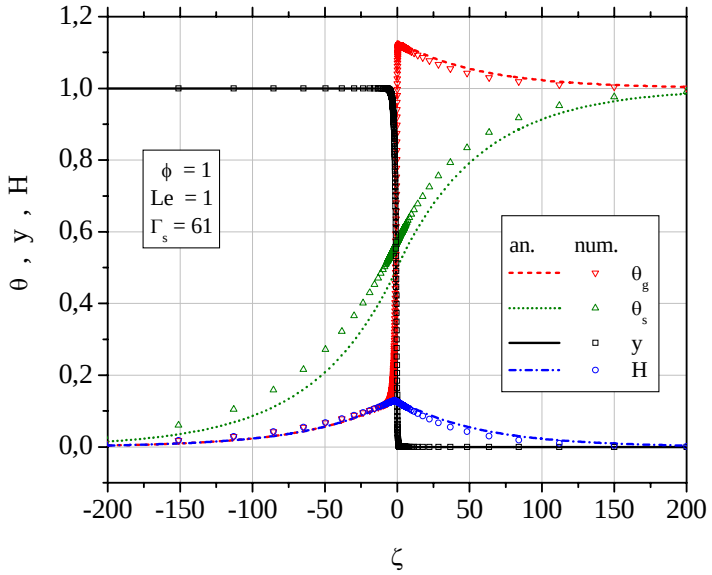

Figure 2. Non-dimensional gas and solid temperatures, fuel fraction profile and excess enthalpy distribution for a flame within a porous media with $\Phi = 1$, Le = 1 and $\Gamma_s = 61$obtained from numerical and analytical solutions.

The analytical solution under predicts θ_g and H for $\zeta < 0$ and over predicts them for $\zeta > 0$. The concentration profile is well reproduced except for values of ζ near the origin because the analytical solution is not able to predict the fuel diffusion downstream of the flame. The analytical solution also over predicts the maximum value of H and θ_g.

Figures (3) and (4) show solutions for Lewis number equal to 2 and 0.5 respectively. For both cases the analytical solution over predicts θ_g at the origin. The excess enthalpy in the flame region near the origin is amplified for Le > 1 and is reduced for Le < 1 reaching negative values (defect of enthalpy) for Le < 0.67.

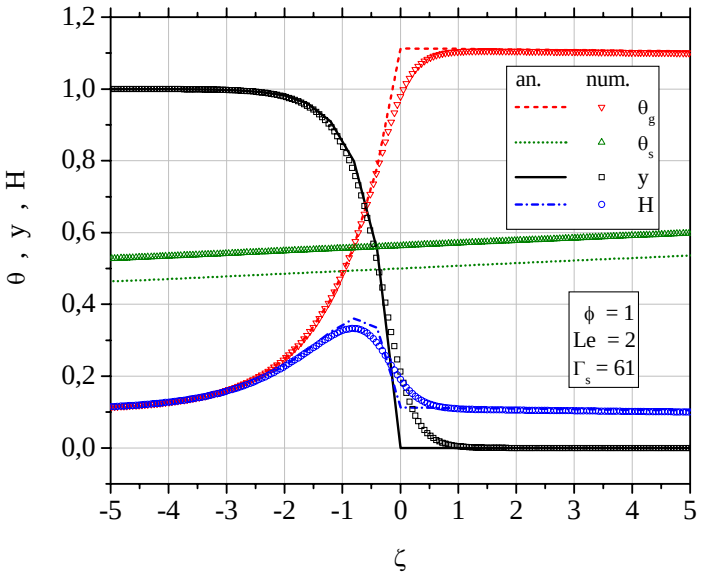

Figure 3. Non-dimensional gas and solid temperatures, fuel fraction profile and excess enthalpy distribution for a flame within a porous media with $\Phi = 1$, Le = 2 and $\Gamma s = 61$.

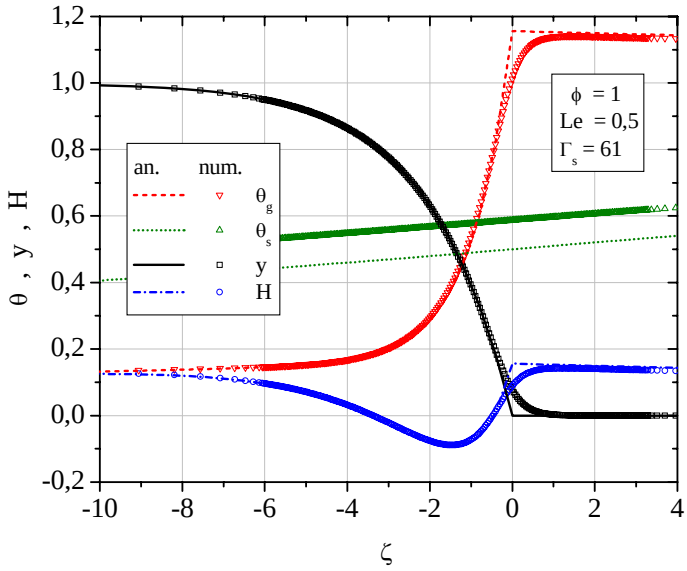

Figure 4. Non-dimensional gas and solid temperatures, fuel fraction profile and excess enthalpy distribution for a flame within a porous media with $\Phi = 1$, Le = 0.5 and $\Gamma_s = 61$.

Figures (5) presents the source terms of the excess enthalpy equation, Eq.(11), for a flame with $\Phi = 1$, Le = 0.5 and $\Gamma s = 61$. The source term corresponding to the Le $\neq 1$ effect (S_{ff}) is negative for $\zeta < -0.5$ and positive for $\zeta > -0.5$, making the flame to present defect of enthalpy in the reaction zone. The source term corresponding to the porous medium effect (S_{pm}) is positive for $\zeta < -0.8$ and negative for $\zeta > -0.8$, making the H profile to present excess enthalpy all over the domain. The S_{ff} source is dominant in the reaction zone and the S_{pm} term is dominant elsewhere. The H profile showed in Fig.(4) is the result of the superposition of these two effects.

The qualitative agreement between numerical and analytical solutions is poor for the S_{ff} term because of the poor approximation used for the y profile. The behavior of the S_{pm} term is well predicted by the analytical solution unless close to the origin.

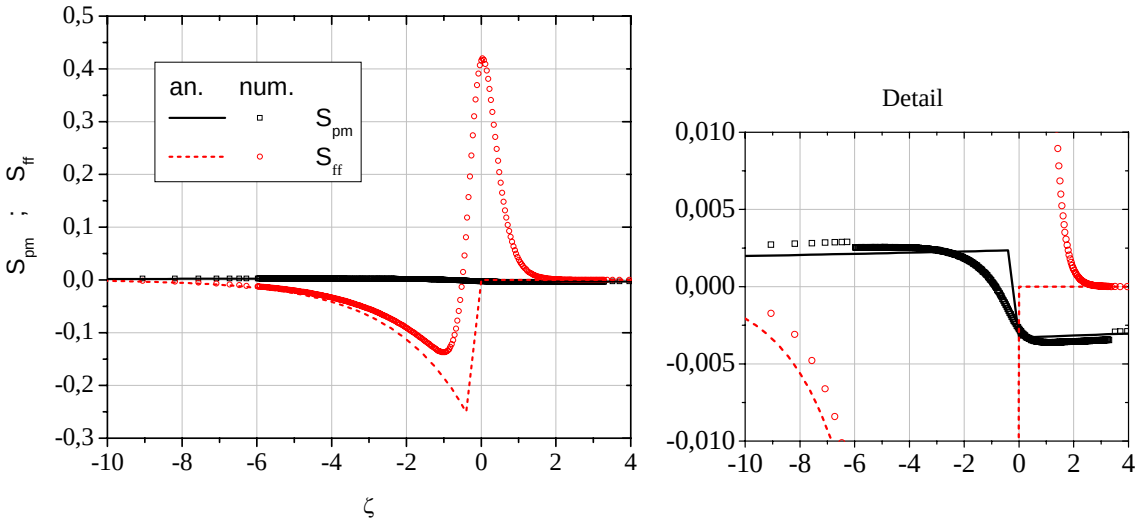

Figure 5. Source terms of excess enthalpy equation - Eq.(11) for a flame with $\Phi = 1$, Le = 0.5 and $\Gamma s = 61$.

4.2. Excess Temperature

Figure (6) shows the peak value of the H equation H_{max} (or H_0) and the superadiabatic flame temperature θ_{sup} as a function of the Lewis number with $\Phi = 1$ and $\Gamma_s = 61$. We can observe that H_{max} increases with the Lewis number while θ_{sup} decreases. This seems to be caused by the gas diffusion downstream of the flame which is enhanced when Le < 1. Figure (7) shows H_{max} and θ_{sup} as a function of the ratio between the solid and gas thermal conductivities Γ_s with $\Phi = 1$ and Le = 1. Both H_{max} and θ_{sup} increase with Γ_s. The agreement between numerical and analytical solutions is good in both situations.

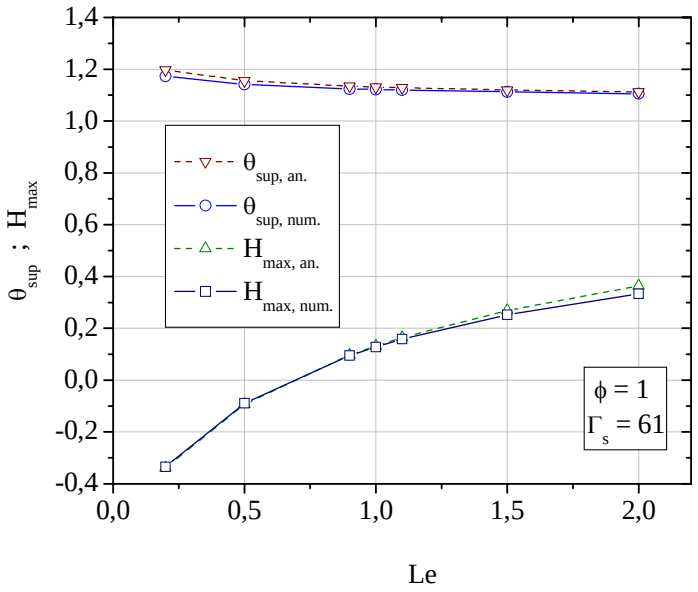

Figure 6. Maximum value of the H equation in the flame zone (H_{max}) as a function of the Lewis number with $\Phi = 1$and $\Gamma s = 61$.

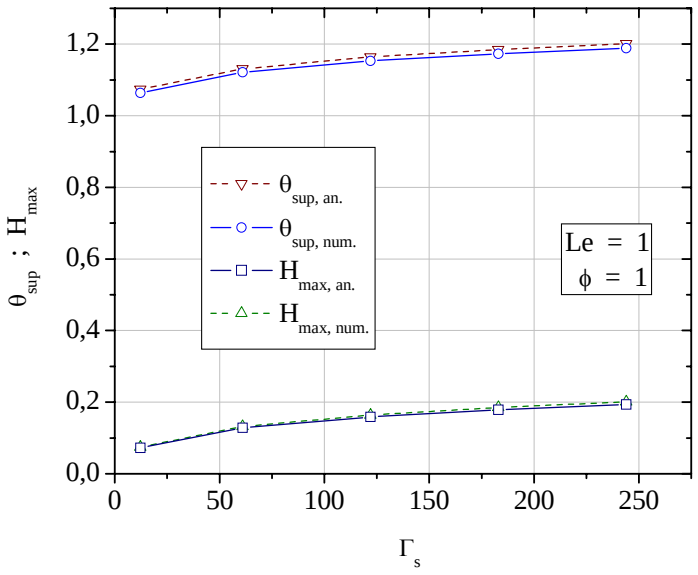

Figure 7. Maximum value of the H equation in the flame zone (H_{max}) as a function of Γ_s with $\Phi = 1$, Le = 1.

Figures (8) and (9) show the variation of the excess enthalpy function with the non-dimensional fuel concentration for flames within a porous medium with Le from 0.5 to 2 and Γ_s from 61 to 244. The adiabatic limit is found when $\theta_g = \theta_{ad} = 1$ is placed in the H equation, giving H = y. This limit is shown as a dash-point line in Figure 8. For points that lie

above this limit, i.e., an H function greater than y, the local non-dimensional gas temperature reaches values above the adiabatic temperature.

When the non-dimensional fuel concentration is equal to unity, i.e., when no fuel has yet been consumed, all flames present an almost vertical excess enthalpy curve. This is due to the enhanced preheating of the gas flow caused by the porous matrix. The cold reactants receive heat from the reaction region achieving an excess enthalpy before entering the flame region. When Le is equal to unity the excess enthalpy presents an almost constant value. When Le < 1 a region of defect enthalpy appears as a result of the S_{ff} term prevailing over the S_{pm} term. However at the end of the reaction region the temperature still reaches an excess value because the S_{ff} term effect is negligible outside the reaction zone. In the other hand, when Le > 1, the excess enthalpy is amplified in the reaction region by the S_{ff} term. In the detail of Fig.(8) it is possible to see clearly that lower Lewis numbers lead to higher maximum enthalpy at y = 0 which results in higher superadiabatic flame temperatures – see Fig.(6). Figure (9) shows that the excess enthalpy also increases with Γ_s leading again to higher superadiabatic flame temperatures as is shown in Fig.(7).

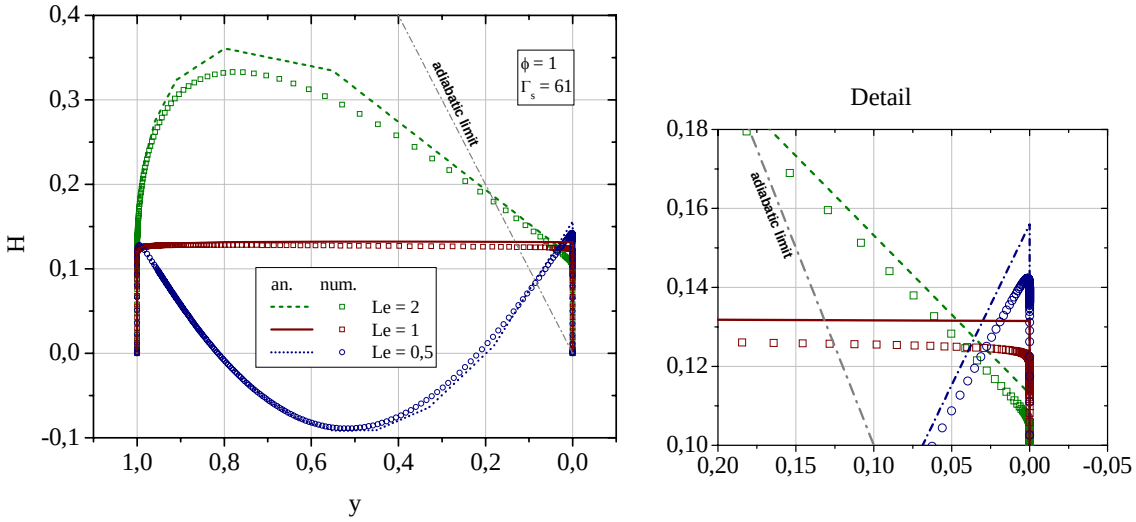

Figure 8. Excess enthalpy as a function of the non-dimensional fuel concentration for various Lewis numbers.

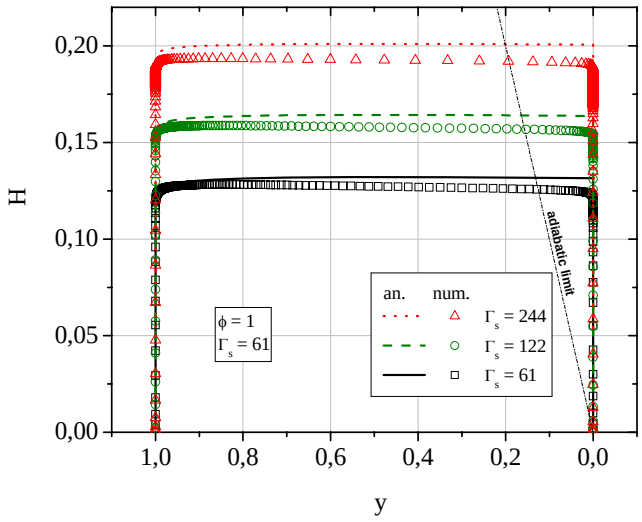

Figure 9. Excess enthalpy as a function of the non-dimensional fuel concentration for various conductivity ratios Γ_s.

The analytical and numerical results show again a good qualitative agreement although the defect or excess enthalpy is always amplified by the analytical solution.

The model presented was able to describe the main aspects of the inner structure of the flame and also of quantify the excess enthalpy effect observed in a porous medium and describe the main variables that affect the value reached for

the maximum temperature. Given the extreme simplicity of the solution, the model is very promising as a strong candidate for a subgrid model for the flame within a porous medium.

5. Conclusions

The excess enthalpy in flames within porous media is analyzed to access the amount of excess temperature above adiabatic temperature originated by the presence of the porous matrix and the factors that affect it. This analysis is based on the excess enthalpy function previously defined in the literature. Approximations for the fuel and solid temperature profiles are used to obtain an approximated analytical solution for the excess enthalpy distribution along the flame. The results are compared with numerical calculations. The main conclusions are:

- The analytical solution shows a good qualitative agreement with the numerical results for the non-dimensional fuel concentration and solid and gas non-dimensional temperature profiles when fed with the numerical flame speed.
- The flame speed calculated by the analytical model depends strongly on the profiles assumed for the fuel mass fraction and solid temperature. Therefore, here, the flame speed is considered known and the values calculated from the numerical solutions are used. This implies that the use of this model as a sub-grid model in future computations of complex flames will require improvements, or an additional, perhaps, empirical model for the local flame speed.
- The excess enthalpy in the flame region near the interface is amplified for $Le > 1$ and is reduced for $Le < 1$ reaching negative values (defect of enthalpy) for $Le < 0.67$.
- The contribution of the free flame source term S_{ff} is negligible in the flame zone when the Lewis number is very closed to one and is dominant in the other cases. This term accounts for the ratio between the mass and thermal diffusion thicknesses. The porous media source term S_{pm} prevails over the S_{ff} term outside the reaction region and leads the gas phase to superadiabatic temperatures. The total amount of excess temperature is the result of a balance between these two terms.
- For all cases there is a region of gas temperatures above the adiabatic temperature, i.e., there is a region of excess temperature. This region is identified in a plot of H against the nondimensional fuel fraction y.
- The superadiabatic temperature increases with Γ_s but decreases with Le. The Γ_s effect is due to the enhancement of the heat recirculation through solid conductivity. The Le effect is due to the fuel concentration at the end of the reaction region when $Le < 1$.
- The necessary condition for reaching gas temperatures above the adiabatic temperature is $\Gamma_s > 1$ combined to a finite interfacial heat transfer coefficient. The first is responsible for the enhanced thermal diffusion when compared to the mass diffusion and the second is responsible for a volumetric heating of the gas phase then increasing the excess enthalpy.

In the sequence of this work, this model is being improved and adapted to be used in complex three-dimensional computations of flames within porous media.

6. Acknowledgement

The authors acknowledge the financial support of the FINEP/RedeGasEnergia through a 2001 CTPETRO grant and the program ANP PRH-09/MECPETRO for the constant support in the form of undergraduate and graduate scholarships. The important contribution of Dr. Fernando Fachini Filho from INPE, Cachoeira Paulista, SP, in helping to define the appropriate characteristic scales in this problem, leading to an important improvement from the formulation used in previous publications, is also greatly appreciated.

7. References

Babkin, V.S., Wierzba, I. and Karim, G.A., 2003, “The Phenomenon of Energy Concentration in Combustion Waves and Its Applications”, Chemical Engineering Journal, Vol.91, pp. 279-285.

Bielert, U. and Sichel, M., 1998, “Numerical Simulation of Premixed Combustion Processes in Closed Tubes”, Combustion and Flame, Vol. 114, pp.397-419.

Echigo, R., 1991, “Radiation Enhenced/Controlled Phenomena of Heat and Mass Transfer in Porous Media”, ASME/JSME Thermal Engineering Proceedings, Vol.4, pp. 21-32.

Fu, x., Viskanta, R. and Gore, J.P., 1998, “Measurement and Correlation of Volumetric Heat Transfer Coefficients of Cellular Ceramics”, Experimental Thermal and Fluid science, Vol.17, pp. 285-293.

Howell, J.R., Hall, M.J. and Ellzey, J.L., 1996, “Combustion of Hidrocarbon Fuels Within Porous Inert Media”, Progress in Energy and Combustion Science, Vol.22, pp. 121-145.

Möβauer, S., Pickenäcker, O., Pickenäcker K. and Trimis, D., 1999, “Application of the Porous Burner Technology in Energy- and Heat-Engineering”, V International Conference on Technologies for a Clean Air Environment, Lisbon.
Oliveira, A.A.M. and Kaviany, M., 2001, “Nonequilibrium in the Transport of Heat and Reactants in Combustion in Porous Media”, Progress in Energy and Combustion Science, Vol.27, pp. 523-545.
Oijen, J.A., Lammers, F.A., De Goey, L.P.H., “Modelin of Complex Premixed Burner Systems by Using Flamelet-Generated-Manyfolds”, Combustion and Flame, Vol. 127, pp.2124-2134.
Saharaoui, M. and Kaviany, M., 1994, “Direct Simulation vs Volume-Averraged Treatment of Adiabatic, Premixed Flame in a Porous Medium, 2001, “International Journal of Heat and Mass Transfer, Vol.17, No.18, pp. 2817-2834.
Wichman, I.S. and Vance, R., 1997, “A Study of One-Dimensional Laminar Premixed Flame Annihilation”, Combustion and Flame, Vol.110, pp. 508-523.
Williams, F., 1985, "Combustion Theory the Fundamental Theory of Chemically Reacting Flow Systems", Perseus Publishing; 2nd edition.
Bielert, U. and Sichel, M., 1998, “Numerical Simulation of Premixed Combustion Processes in Closed Tubes”, Combustion and Flame, Vol. 114, pp.397-419.

8. Nomenclature

a	temperature exponent in the reaction rate equation
A	pre-exponential factor
c_p	specific heat
D	mass diffusivity
Da	Damköhler number
D_p	mean pore diameter
E_a	activation energy
h	convection coefficient $h = S_{gs}(Nu\lambda_{g,m}/D_p)$
H	excess enthalpy function $H = y + \theta - 1$
Le	Lewis number $Le = \lambda/\rho D c_p = \alpha_g/D$
Le_s	modified Lewis number $Le_s = Le\Gamma_s$
L_q	lengh of the burner
N	heat transfer between the phases parameter
Nu	Nusselt number
Q	chemical heat release
R_g	universal gas constant
Re_D	Reynolds number $Re = \rho u D_p/\mu$
S_{gs}	specific area between the phases
T	temperature
u	flow velocity
W	non dimensional reaction rate
y	reduced fuel mass fraction $y = Y_F/Y_{F,n}$
Y_F	fuel mass fraction

Greek Symbols

α	enthalpy ratio $\alpha = 1-T_n/T_r$ or thermal diffusivity
β	Zeldovich number $\beta = \alpha(E_a/R_gT_r)$
ε	solid matrix porosity
λ	thermal conductivity
ν_F	fuel stoichiometric coefficient
ρ	density
μ	viscosity
θ	non-dimensional normalized temperature $\theta = (T_g-T_n)/(T_r-T_n)$
Φ	equivalence ratio
Γ_s	conductivity ratio $\Gamma_s = \lambda_s/\lambda_g$
ζ	spatial coordinate $\zeta = \int_0^x \frac{\rho_n u_n c_p}{\lambda_s} dx$

Subscripts

e	effective
g	gas phase
i	ignition
m	molecular
max	maximum
n	non-reacted
r	reacted
s	solid phase

9. Responsibility Notice

The authors are the only responsible for the printed material included in this paper.